

Linear and Nonlinear Shear Rheology of a Marginally Entangled Ring Polymer

Zhi-Chao Yan,[†] Salvatore Costanzo,^{†,‡} Youncheol Jeong,[§] Taihyun Chang,[§] and Dimitris Vlassopoulos^{*,†,‡}

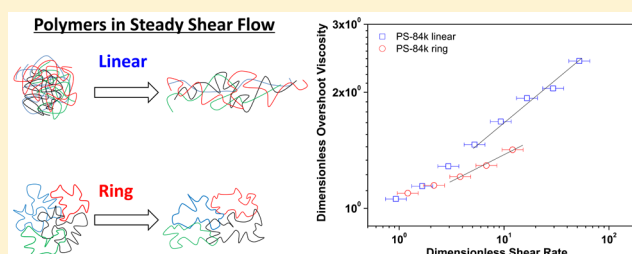
[†]Institute of Electronic Structure and Laser, FORTH, Heraklion 71110, Crete, Greece

[‡]Department of Materials Science & Technology, University of Crete, Heraklion 71003, Crete, Greece

[§]Division of Advanced Materials Science and Department of Chemistry, Pohang University of Science and Technology, Pohang 37673, Korea

Supporting Information

ABSTRACT: We present systematic, unique linear and nonlinear shear rheology data of an experimentally pure ring polystyrene and its linear precursor. This polymer was synthesized anionically and characterized by interaction chromatography and fractionation at the critical condition. Its weight-average molar mass is 84 kg/mol; i.e., it is marginally entangled (entanglement number $Z \approx 5$). Its linear viscoelastic response appears to be better described by the Rouse model (accounting for ring closure) rather than the lattice-animal-based model, suggesting a transition from unentangled to entangled ring dynamics. The failure of both models in the terminal region may reflect the remaining unlinked linear contaminants and/or ring–ring interpenetration. The viscosity evolution at different shear rates was measured using a homemade cone-partitioned plate fixture in order to avoid edge fracture instabilities. Our findings suggest that rings are much less shear thinning compared to their linear counterparts, whereas both obey the Cox–Merz rule. The shear stress (or viscosity) overshoot is much weaker for rings compared to linear chains, pointing to the fact that their effective deformation is smaller. Finally, step strain experiments indicate that the damping function data of ring polymers clearly depart from the Doi–Edwards prediction for entangled linear chains, exhibiting a weak thinning response. These findings indicate that these marginally entangled rings behave like effectively unentangled chains with finite extensibility and deform much less in shear flow compared to linear polymers. They can serve as guideline for further investigation of the nonlinear dynamics of ring polymers and the development of constitutive equations.



1. INTRODUCTION

Despite recent progress,^{1–7} the fundamental understanding of the rheology of ring polymers is an outstanding challenge. Their lack of free ends sets them apart from other types of polymers as the adjustment of chain conformation in response to an external stimulus is very different.⁸ The early works of Roovers,^{9,10} McKenna,¹¹ and Semlyen¹² and their co-workers showed that rings are unique as their properties are quantitatively different from those of their linear precursors. However, significant discrepancies among ring data remained, rendering the field open and controversial. Recently, it has been demonstrated that entangled rings can be adequately purified by means of fractionation by liquid chromatography at the critical condition (LCCC)¹³ and in that case their stress relaxes self-similarly,^{1,5} i.e., in a qualitatively different way from linear polymers. This is successfully described by the lattice-animal model and others in the same spirit^{14–21} or molecular dynamics simulations.⁴ These new results have led to the conclusion that contamination due to unlinked linear precursor which was present in the ring sample fractionated by traditional SEC means was the main reason for the controversies in the 1980s.^{1,22,23} Therefore, LCCC is the current state-of-the-art

approach to remove the residual linear contaminants from ring polymers.²⁴ LCCC relies on a balance of the entropic size exclusion and enthalpic interaction of polymers with porous packing materials in the LC column.

From the above one can conclude that by now it is established that entangled pure ring polymers do not exhibit plateau modulus but a power-law stress relaxation instead, with a power-law exponent of about 0.4, and a faster terminal relaxation compared to their linear precursors.^{1,2,4,5} However, experiments suggest that the terminal response can be more complicated and may not be fully captured by the available models, being in fact characterized by a slow mode, in addition to ring relaxation.² Whereas this remains an open question, there is growing evidence linking the slow mode to tiny fraction of unlinked linear polymers (which can be either leftovers from the initial reaction product that are not resolved by LCCC or the result of thermal fatigue after continuous measurement, leading to rupture of the ring's bond) which thread rings and

Received: December 7, 2015

Revised: January 31, 2016

Published: February 5, 2016

possible ring–ring mutual threading.^{22,25–28} On the other hand, for ring polymers of low molar mass the lattice-animal model overestimates the terminal region substantially.⁵ Conversely, a Rouse model appropriately modified to account for the linking of the two ends of a chain is much more accurate in the description of the terminal region.^{5,29} Given the difference in conformation and the related difference in response to topological constraints as outlined above, the transition from unentangled to entangled dynamics is not necessarily signaled by the same critical molar mass in linear and ring polymers. Indeed, Doi et al.⁵ showed recently that up to about 90 kg/mol a polystyrene ring is better described by a Rouse-ring model (albeit not perfectly), whereas its linear precursor by the standard tube-based model.³⁰

The nonlinear rheology of ring polymers has been virtually unexplored. Several modeling and simulation works demonstrated that ring polymers differ from their linear counterparts also in nonlinear rheology.^{31–33} Rouse ring polymers do not exhibit shear thinning of damping in step strain.³² On the other hand, simulations of single rings in solution (where hydrodynamic effects matter), accounting for finite extensibility, have shown the occurrence of shear thinning.^{31,33–35} However, there are no virtually experimental studies on nonlinear ring polymer rheology, yet they are necessary in order to advance our understanding of the molecular structural changes under flow. Only very recently Schroeder and co-workers reported on the transient planar elongational flow of a single large DNA ring, observed at the stagnation point of a cross-slot microfluidic trap.³⁶ They found that rings stretch less and differently from linear chains. Besides the extremely limited availability of purified rings (LCCC fractionation is very time-consuming), measuring the nonlinear shear flow behavior of polymer melts is very challenging due to flow instabilities such as edge fracture and wall slip.^{37–40} In order to address this issue, a homemade cone partitioned-plate (CPP) geometry was developed and implemented in different rheometers.^{40–42} We have tested the reliability of our CPP geometry using linear and branched polymers.^{42–44} In addition to step shear rate, nonlinear step strain tests provide important information on nonlinear shear stress relaxation.^{45–52} Hence, step shear rate and stress relaxation tests constitute powerful experimental tools to sensitively detect the response of ring polymers in nonlinear shear flow.

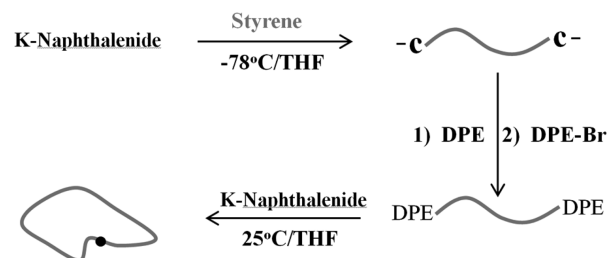
From the above it is evident that the intermediate molar mass regime between unentangled and well-entangled behavior deserves further investigation, and more importantly, the nonlinear shear rheology of pure rings should be explored as it is still at an embryo stage. We call this molar mass regime “marginally entangled” and use a well-characterized polystyrene in order to address the above challenge, i.e., study of its linear and nonlinear shear rheology.

This article is structured as follows. We first describe the material information and the experimental methods, with particular emphasis on the LCCC characterization which represents the key for this (and any relevant) study. Then, the linear viscoelasticity and their comparison with the theoretical predictions are presented. The nonlinear rheological results, including data from step shear rate and nonlinear stress relaxation tests, are reported along with the explanation of their molecular origin. Finally, concluding remarks are summarized.

2. MATERIALS AND METHODS

2.1. Polymers. The polystyrene (PS) ring sample is synthesized by ring closure of telechelic polystyrene which was prepared in THF by anionic polymerization using potassium naphthalenide as an initiator. The synthetic scheme is shown in Scheme 1.

Scheme 1. Synthetic Scheme of Polystyrene Ring



The anionic ends of PS were end-capped with diphenylethylene (DPE) first and then further reacted with 1-(4-(3-bromopropyl)-phenyl)-1-phenylethylene (DPE-Br) to make a telechelic DPE-ended PS. DPE-Br was prepared and purified according the procedure in the literature.⁵³ The ring closure of the telechelic PS was carried out in dilute THF solution (0.1% w/v) by potassium naphthalenide.⁵⁴ As-synthesized ring PS contains a significant amount of byproducts (various linear adducts as well as multiple rings), and it is purified by fractional precipitation first to remove most of the high MW adducts. Then it is subjected to LCCC fractionation to obtain single ring PS with high purity.

The ring polymer is very sensitive to the linear contamination. A tiny amount of linear component added to ring systems will induce a dramatic change in their rheological behavior.¹ On the other hand, the conventional liquid chromatography cannot effectively purify the ring sample. Here, the ring sample is purified by LCCC fractionation.¹³ The LCCC technique can effectively purify the ring sample, making the residual linear contamination hardly detectable in any analysis techniques including SEC, LCCC, and MALDI-MS.^{13,55} The SEC chromatogram in Figure 1a shows the comparison between the elution curves before and after LCCC fractionation. The results clearly indicate a very effective purification of the ring polymer from the residual linear precursor. Figure 1b shows the comparison between the chromatograms of the fractions of ring polymer and its linear precursor that had been separated by LCCC. The elution peak of the ring sample corresponds to a larger value of the elution volume with respect to the linear sample. This corroborates the known fact that due to molecular structure, ring polymers have smaller size compared to linear polymers of the same M_w . The weight-average molar mass, M_w , and the polydispersity, M_w/M_n , of the ring (coded as PS-84k ring) polymer determined by SEC-light scattering detection⁵⁶ were 84 kg/mol and 1.003, respectively.

For comparison, we also used the linear polystyrene precursor (same molar mass), with code PS-84k linear, as well as a higher molar mass (185 kg/mol) linear polystyrene (obtained from Polymer Source, Canada), with code PS-185k linear. In addition, we used two blends of ring and linear polystyrenes, as described in the next section: (i) molar mass 84 kg/mol for both components, with the fraction of the linear being 85%; (ii) molar mass 198 kg/mol (code PS-198k ring) for the ring (from ref 1) and 450 kg/mol for linear (code PS-450k linear), with the fraction of the latter being 0.001. The reason for using the blends is to test the response of a network formed by linear chains threading rings when their fraction is extremely small. To this end, we used a blend consisting of the tested ring polymer (PS-84k ring) and its precursor and another one with larger molar masses for both ring and linear. For the latter in particular, we used a double molar mass compared to the ring, but note that a smaller one, say equal, would work as well.

2.2. Methods. Rheological measurements were performed on a strain-controlled ARES rheometer (TA Instruments, USA) equipped

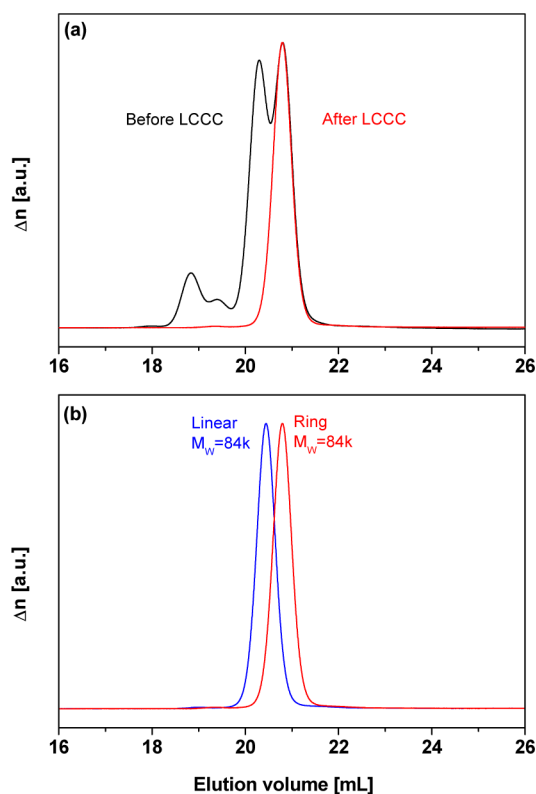


Figure 1. (a) SEC chromatograms of ring products before (black) and after (red) LCCC fractionation. (b) SEC chromatograms of linear precursor (blue) and pure ring (red) after LCCC fractionation.

with a force rebalance transducer (2KFRTN1). Since, as already discussed, nonlinear shear measurements are prone to flow instabilities like edge fracture and wall slip, we used a newly designed homemade cone partitioned-plate geometry (CPP). Details on the CPP operation, as adopted for the ARES rheometer, can be found in ref 42. Here, we introduced several design improvements that allowed us to carry out start-up shear flow measurements in a more controlled fashion. The new fixture is schematically shown in Figure 2. One of its major

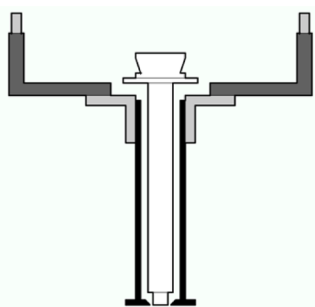


Figure 2. Schematic front view of CPP geometry: inner tool (white), outer corona (black), translation stages (light gray), and bridge (dark gray).

advantages is that it has superior temperature control. More specifically, a homemade stainless steel plate with 6 mm diameter is used along with a shaft of diameter 10 mm, leaving a large gap between the shaft of the tool and the oven. This gap allowed building a coaxial hollow cylinder around the inner tool in such a way that the whole geometry could fit into the ARES convection oven, ensuring a very accurate temperature control (± 0.1 °C). The hollow cylinder holds the outer partition at its bottom base, avoiding any contact with the inner tool. The outer partition consists of a stainless steel corona with

an outer diameter of 20 mm and an inner diameter of 6.16 mm; thus, the gap between the partitions is around 80 μm . The hollow cylinder is fixed to the head of the rheometer by means of a hollow bridge equipped with vertical and horizontal homemade translation stages. The latter permit both vertical and horizontal alignment of the outer partition with respect to the inner one. Once the geometry is aligned, it can be fixed by means of horizontal and vertical screws. All pieces of the CPP are made of the same stainless steel in order to have the same thermal expansion coefficient. For this reason, the error in the alignment of the partitions induced by thermal variations was found negligible. A standard 25 mm diameter cone with an angle of 0.1 rad and a truncation of 0.051 mm was used as bottom geometry.

For the step-strain measurements, a different cone–plate geometry, with cone angle of 0.04 rad and without the CPP setup, was employed. It was found that this geometry can provide reliable, artifact-free measurements.^{51,52} The experimentally available shear strain range is obtained based on the formula for the shear strain in a cone and plate geometry, namely $\gamma = \Omega/\varphi$, with γ being the strain units, φ being the cone angle, and Ω being the angular displacement limits of the motor.⁵⁷ Considering the instrumental limitations of Ω (0.00005–0.5 rad for the ARES rheometer used), higher shear strains can be achieved for small cone angles φ . For example, for a 0.1 rad cone, the strain unit range of ARES is 0.0005–5; for a 0.04 rad cone, the strain unit range is 0.00125–12.5. Therefore, we used the particular angle (0.04 rad) in order to reach a high strain value of $\gamma = 10$ (strain units). The small plate diameter (4 mm) was chosen in order to protect the transducer from abnormal resonance due to compliance problems caused by both the small cone angle⁵⁸ and the high stiffness of the sample at near- T_g temperatures.

3. EXPERIMENTAL RESULTS

3.1. Linear Viscoelasticity. The master curves of the dynamic moduli as a function of shifted frequency for the PS-84k ring polymer, its linear precursor, and their mixture with 85% linear composition are shown in Figure 3a at the reference temperature of $T_{\text{ref}} = 150$ °C. A moderate entanglement plateau can be observed for the linear polymer ($Z \approx 5$). The respective ring polymer exhibits power-law dynamics and a shorter relaxation time. We note also that the terminal slopes are virtually reached for this ring, which is usually not the case for rings of higher molar mass.^{1,2,5} This complies with the suggestion that the slow mode in ring relaxation is primarily attributed to unlinked linear contaminants (not resolved by LCCC), whose fraction is even less significant at lower molar mass (due to higher linking probability in the reaction process).² These features are consistent with the previous findings.^{1,5} The rheological master curve of the mixture with 85% linear component virtually overlaps with the linear data at frequencies higher than the terminal $G' - G''$ crossover, ω_c . On the other hand, below ω_c , the mixture exhibits a broadening of the terminal region and hence a higher viscosity. This reflects the threading of the rings by the linear chains, widely reported in experimental and simulation works in the literature.^{9–11,23}

In Figure 3b, the horizontal shift factor a_T used to create the master curves is plotted against temperature. In the same plot, indicative a_T data from different polystyrene architectures at the same reference temperature are shown: linear $M_w = 185$ kg/mol,⁴² ring 198 kg/mol,¹ comb C642 ($M_{w,\text{backbone}} = 275$ kg/mol, $M_{w,\text{branch}} = 47$ kg/mol, 29 branches)⁵⁹ and H-3 macromolecules ($M_{w,\text{backbone}} = 146$ kg/mol, $M_{w,\text{branch}} = 132$ kg/mol, four outer branches).^{60,61} The good overlap observed indicates that macromolecular architecture does not affect the shift factors for these studied molar masses (corresponding to the same, M_w -independent T_g). The WLF fit (solid curve) of all data results in values of the coefficients $C_1 = 7.2$ and $C_2 = 103$ K, at T_{ref} . The vertical shift factors b_T reflect the density

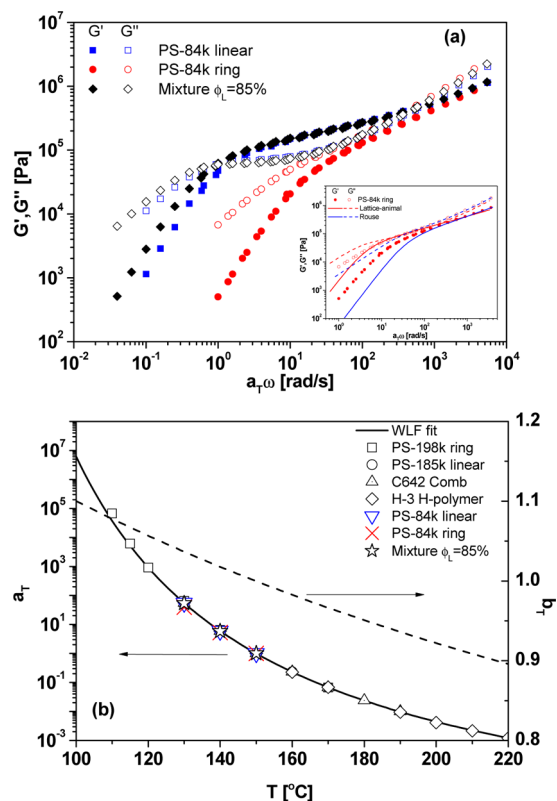


Figure 3. (a) Master curves for the storage G' and loss G'' moduli as a function of shifted frequency of linear precursor PS-84 linear (blue squares), the purified ring PS-84k ring (red circles), and their mixture with $\phi_L = 85\%$ (black diamonds) at a reference temperature $T_{\text{ref}} = 150$ °C. Inset: the data of PS-84k ring are compared with predictions from the lattice-animal model (red lines) and Rouse-ring model (blue lines), respectively (see text). (b) Horizontal a_T and vertical b_T shift factor at the reference temperature $T_{\text{ref}} = 150$ °C of linear, ring, and mixture samples. Also plotted are shift factors from other polystyrenes, including linear ($M_w = 185$ kg/mol),⁴² PS-198k ring,¹ comb C642 ($M_{w,\text{backbone}} = 275$ kg/mol, $M_{w,\text{branch}} = 47$ kg/mol, 29 branches),⁵⁹ and H-macromolecules ($M_{w,\text{backbone}} = 146$ kg/mol, $M_{w,\text{branch}} = 132$ kg/mol, four outer branches).^{60,61} The solid line is the fit with the WLF equation. The dashed line corresponds to the vertical shift factors b_T and follows the density compensation (see text).

compensation.⁶² The temperature dependence of density $\rho(T)$ (in g/cm^3) was taken from ref 63: $\rho(T) = 1.2503 - 6.05 \times 10^{-4}(273.15 + T)$.

To examine the relaxation mechanism of ring polymers quantitatively, both lattice-animal^{14–16} and Rouse-ring^{5,29} models were tested with respect to their ability to describe the experimental data, complemented by an empirical high-frequency relaxation mode (simply for fitting purposes) corresponding to the rubber-to-glass transition.^{5,64,65} The frequency-dependent storage G' and loss G'' moduli based on the lattice-animal model are given by the following equations:^{1,7,14}

$$G'(\omega) = G_N^0 \frac{M_e}{M} \left(\frac{\omega}{\beta} \right)^{2/5} \frac{\Gamma\left(\frac{3}{5}\right)}{\left[\left(\frac{\beta}{\omega} \right)^2 + 1 \right]^{3/10}} \sin \left[\frac{3}{5} \arctan \left(\frac{\omega}{\beta} \right) \right] \quad (1)$$

$$G''(\omega) = G_N^0 \frac{M_e}{M} \left(\frac{\omega}{\beta} \right)^{2/5} \frac{\Gamma\left(\frac{3}{5}\right)}{\left[\left(\frac{\beta}{\omega} \right)^2 + 1 \right]^{3/10}} \cos \left[\frac{3}{5} \arctan \left(\frac{\omega}{\beta} \right) \right] + A\omega \quad (2)$$

with M the molar mass, G_N^0 the plateau modulus of the linear precursor, M_e the molar mass between entanglements, τ_e the relaxation time of an entanglement segment, $\beta = (M_e/M)^{2.5}/\tau_e$, and Γ the gamma function. The molecular parameters at 150 °C, $\tau_e = 5.3 \times 10^{-3}$ s, $M_e = 17$ kg/mol, and $G_N^0 = 0.18$ MPa, were taken from the linear polystyrene data at 170 °C¹ using the horizontal and vertical shift factors in Figure 3b. The term of $A\omega$ accounts for the high-frequency contribution to G'' .^{64,65} The value of A is 304 Pa·s at 150 °C, shifted from the reported data at 180 °C.^{64,65} The high-frequency contribution to G' is negligible.

The Rouse-ring prediction for rings can be expressed by the following equations:^{5,29}

$$G'(\omega) = G_N^0 \frac{2M_e}{M} \sum_{p \geq 1} \frac{\omega^2 \tau_p^2}{1 + \omega^2 \tau_p^2} \quad (3)$$

$$G''(\omega) = G_N^0 \frac{2M_e}{M} \sum_{p \geq 1} \frac{\omega \tau_p}{1 + \omega^2 \tau_p^2} + A\omega \quad (4)$$

with

$$\tau_p = \frac{\tau_p}{p^2} \quad \text{and} \quad \tau_{\text{ring}} = \frac{\tau_{\text{linear,Rouse}}}{4} \quad (5)$$

with p the mode number, τ_p the p th Rouse relaxation time, and τ_{ring} the longest Rouse relaxation time of the ring sample. Note that due to the boundary condition for the ring (no free ends), its mode structure is different and the lowest mode that exists in a linear Rouse chain is absent. Instead, the lowest ring mode has half wavelength compared to linear, and consequently τ_{ring} is estimated as 1/4 of the Rouse relaxation time of the respective linear chain with the same M , $\tau_{\text{linear,Rouse}}$.^{5,29,32} The latter was determined from $\tau_{\text{linear,Rouse}} = \tau_e Z^2$,⁶⁶ with $\tau_e = 5.3 \times 10^{-3}$ s as mentioned above and $Z = 5$, yielding 0.13 s. The other molecular parameters, like M_e and G_N^0 , are the same with that used in the lattice-animal prediction.

The inset of Figure 3a depicts the frequency-dependent moduli of PS-84k ring along with the predictions from the lattice-animal (eqs 1 and 2) and Rouse-ring (eqs 3–5) models. Both models capture the high-frequency response, with the Rouse ring being slightly better, suggesting that this polystyrene ring with $M_w = 84$ kg/mol is marginally entangled. This result is in good agreement with that of ref 5, where a molar mass of 90 kg/mol was identified as that marking the transition to entangled behavior of polystyrene rings. At intermediate frequencies, G' and G'' exhibit a power-law relaxation with an exponent of 0.52, consistent with the Rouse-ring prediction but larger than that the lattice-animal model (0.4). On the other hand, for molar masses above 90 kg/mol, polystyrene rings display a weaker power-law exponent, almost identical to the lattice-animal prediction, over more than 2 decades in frequency.^{1,2,5} In the terminal regime, the lattice-animal model overestimates the longest relaxation time for PS-84k ring, in contrast to its high molar mass counterparts.^{1,5} In the latter case, the underestimation of the experimental data by the model was attributed to ring–linear and ring–ring threading events which were not considered, as discussed in the

Introduction. In the present case of PS-84k ring, the lattice-animal model overestimates the terminal relaxation while the Rouse-ring model underestimates it. This reflects the transitional state of this particular polymer where (much as in the similar situation with linear polymers⁶⁷) neither model is entirely adequate. Clearly, the PS-84k ring feels topological constraints but not as severe as in larger molar mass case where double folds (or loopy globules) form. Apart from this scenario, we also note that lower molar mass ring polymers are expected to have lower probability of linear contaminants;² hence, slow modes (that delay terminal response) are weaker compared to higher molar mass rings. On the basis of these considerations, in accord with recent experimental reports on polystyrene rings,⁵ we suggest that the transition from unentangled to entangled ring dynamics occurs at $Z \approx 5$. At this number of entanglements, the presence of free ends leads to a clearly discerned plateau modulus (Figure 3a). Doi et al.⁵ also reported the dependence of the zero-shear viscosity (η_0) on the molar mass. It was found to dramatically change from the Rouse scaling ($\eta_0 \sim M_w$) to a stronger M_w dependence ($\eta_0 \sim M_w^{2.9 \pm 1.0}$) at the crossover $M_w = 90$ kg/mol.⁵ The high- M_w exponent (2.9 ± 1.0) is close to the bare reptation prediction for entangled linear chains⁶⁸ but larger than both the lattice-animal prediction ($\eta_0 \sim M_w^{3/2}$)^{14,16} and a recent loopy globule prediction ($\eta_0 \sim M_w^{5/3}$).¹⁷ Nevertheless, we note that only three points (240 kg/mol from Doi et al.;⁵ 198 and 161 kg/mol from Kapnistos¹) are available above 90 kg/mol, and they are not perfectly consistent probably due to the difference of ring purity. A rigorous and systematic test need more high- M_w ring samples with uniformly high purity. It is tempting to relate these observations to change in molecular conformation of the rings. In fact, recent molecular dynamics simulations show that whereas rings in the melt are relatively compact objects, as molar mass increases they slightly expanded with voids that can be occupied by neighboring rings.³ Further work will be needed however to make a quantitative link.

The above results, along with those already published in the literature with polystyrene rings, can be compiled in Figure 4, which depicts the recoverable compliance J_e as a function of the molar mass M_w . Data are shown for the PS ring sample from

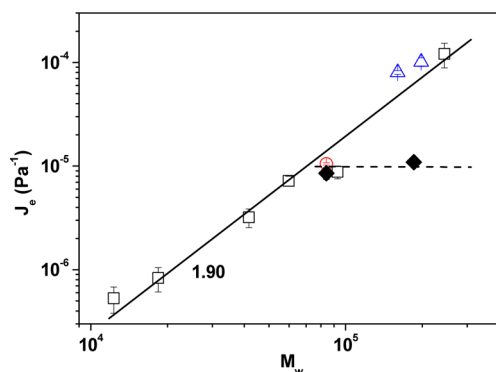


Figure 4. Molar mass dependence of the recoverable compliance, J_e , at the reference temperature $T_{\text{ref}} = 160$ °C for ring polystyrenes from the present study (red open circle), Kapnistos et al. (blue open triangles),¹ and Doi et al. (black open squares).⁵ The black line is the fit to all ring data with slope of 1.90 ± 0.13 . Also plotted are the data of linear polymers (PS-84k linear and PS-185k linear, black closed diamonds) for comparison. The horizontal dashed line is drawn to guide the eye (see text).

the present study, from Kapnistos et al.,¹ and from Doi et al.⁵ In addition, respective data from two PS linear samples as shown for comparison (PS-84k linear and PS-185k linear). To estimate the average values of J_e , we extrapolated the terminal slopes of G' and G'' and used $J_e = (1/\eta_0^2) \lim_{\omega \rightarrow 0} (G'(\omega)/\omega^2)$. In contrast to linear chains, which exhibit a crossover to M_w -independent J_e , the J_e of rings increases continuously even at rather high molar masses (up to about $Z = 15$ entanglements) with a scaling slope of 1.90 ± 0.13 . This result confirms and complements that of Doi et al.,⁵ which is in the spirit of earlier assertions of McKenna and co-workers.^{7,69} In spite of the slight scattering of the data (likely due to difference in ring purity and experimental accuracy), the slope of 1.90 marks a sharply different behavior of rings compared to their linear precursors (for Rouse chains the slope is 1 whereas, as mentioned, for entangled chains it is zero).

3.2. Nonlinear Start-Up Shear Flow Behavior. The transient shear viscosity η^+ as a function of time t for different imposed shear rates $\dot{\gamma}$ at 150 °C is depicted in Figure 5 for PS-84k linear, PS-84k ring, and their mixture with 85% linear. The linear viscoelastic (LVE) envelope lines are shown as well (thick dark lines) to confirm data consistency. The respective lines are calculated by direct transformation of the dynamic master curves according to the empirical Cox–Merz rule⁷⁰ $\eta(\dot{\gamma}) = \eta^*(\omega)|_{\omega=\dot{\gamma}}$ in conjunction with the Gleissle rule⁷¹ $\eta^+(t) = \eta(\dot{\gamma})|_{\dot{\gamma}=1/t}$. Beyond the start-up time of motor, the nonlinear data collapse on the LVE envelope at low times or strains. A deviation of transient viscosity from LVE envelope was observed with increasing shear rate and time. After an overshoot, the transient viscosity reaches its steady-state value. Visual comparison of Figures 5a and 5b, in particular at the highest shear rates which are comparable, indicates the linear PS has more prominent overshoot than the ring PS. Since the overshoot reflects the maximum flow-induced deformation of the polymer, this qualitative observation already implies that the rings experience less deformation than its linear precursors in simple shear flows. This is consistent with the recent experimental observations of Schroeder and co-workers on single DNA ring extension, which is reduced compared to linear DNA.³⁶ However, we note that this analogy is only offered on a qualitative basis in order to emphasize the smaller deformation of rings compared to their linear analogues; it is important to keep in mind that the single DNA of ref 36 is a very different problem from the present melt of PS rings. On the other hand, the ring–linear blend exhibits a transient shear response which is quantitatively very similar to that of linear polystyrene as seen in Figure 5c. Given the fact that even small fractions of linear chains alter the viscoelastic nature of the ring via formation of an effective network,^{1,23} this result is not surprising.

The steady-state viscosity η_{STEADY} , extracted from Figure 5, is plotted against shear rate in Figure 6. The values of η_{STEADY} were taken as the average over the final steady-state portion of the start-up curves. The standard deviation was found to be negligible (less than the symbol size). We observe that the low-shear data reflect the clear differences between rings and linear chains (and their blends) as documented in the literature^{1–5} and discussed above. On the other hand, remarkably, the high-rate data collapse. This important result is in agreement with molecular dynamics simulations of Halverson et al.²³ and shows that the local modes responsible for the behavior in this regime are the same, irrespectively of the architecture (ring, linear, blend).

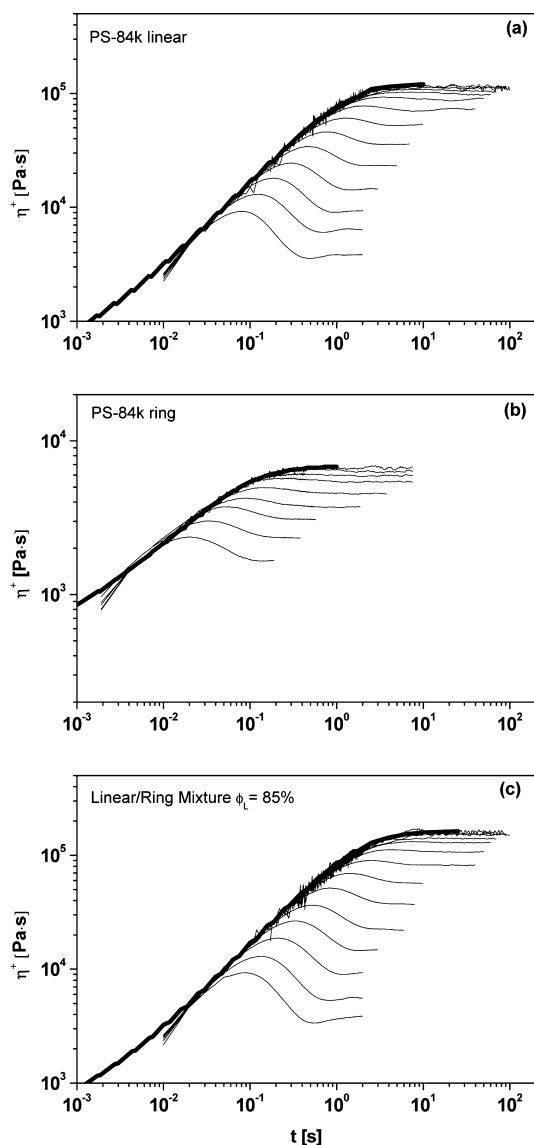


Figure 5. Nonlinear startup shear viscosity η^+ as a function of time t at 150 °C. Data are shown for (a) the PS-84k linear, with shear rates from top to bottom: $\dot{\gamma} = 0.0316, 0.0562, 0.1, 0.178, 0.316, 0.562, 1, 1.78, 3.16, 5.62, 10, 17.8, 31.6,$ and 56.2 s^{-1} ; (b) the PS-84k ring, with shear rates from top to bottom: $\dot{\gamma} = 1.66, 2.96, 5.26, 9.36, 16.6, 29.6, 52.6, 93.6,$ and 166 s^{-1} ; and (c) their mixtures with $\phi_L = 85\%$, with shear rates from top to bottom: $\dot{\gamma} = 0.0316, 0.0562, 0.1, 0.178, 0.316, 0.562, 1, 1.78, 3.16, 5.62, 10, 17.8, 31.6,$ and 56.2 s^{-1} . The LVE envelopes are shown as thick lines in all panels. The PS-84k ring data were obtained at 140 °C at shear rates $\dot{\gamma} = 0.316, 0.562, 1, 1.78, 3.16, 5.62, 10, 17.8,$ and 31.6 s^{-1} and then shifted to 150 °C by using the shift factors in Figure 3b.

Several nonlinear rheological parameters, extracted from Figure 5, can be used in order to further analyze the data. The normalized steady-state shear viscosities (to the zero-shear value) $\eta_{\text{STEADY}}/\eta_0$, the relative peak (maximum) viscosities with respect to the steady state value $\eta_{\text{MAX}}/\eta_{\text{STEADY}}$, and the strains at the peak viscosities γ_{MAX} represent measures of chain deformation in shear flow and are plotted in Figure 7 against the normalized shear rate (Weissenberg number). Here, in addition to the moderately entangled PS-84k linear polystyrene (with $Z \approx 5$), data for a well-entangled PS-185k linear polystyrene (with $Z \approx 11$) are also plotted for comparison.

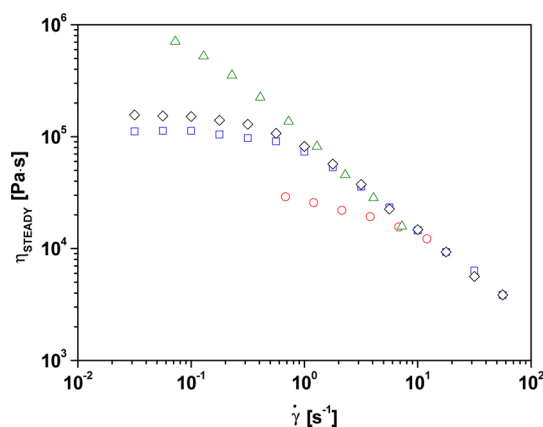


Figure 6. Steady-state viscosity of PS rings, linear chains, and mixtures versus shear rate. Data obtained from Figure 5. Blue squares, red circles, black diamonds, and green triangles correspond to PS-84k linear, PS-84k ring, their mixture with $\phi_L = 85\%$, and PS-185k linear, respectively.

The ratio $\eta_{\text{STEADY}}/\eta_0$ is plotted in Figure 7a as a function of the Weissenberg number $Wi = \dot{\gamma}\tau_d$, with τ_d being the terminal relaxation time, determined by the inverse of the intersection of the extrapolation of the limiting power laws of $G' \sim \omega^2$ and $G'' \sim \omega$.⁷² Note that the determination of τ_d is the main source of the horizontal errors in Wi , hence in error bars in the Figure 7. Also plotted in Figure 7a are LVE envelopes transformed from the linear oscillatory data as a function of the respective Deborah number $De_0 = \omega\tau_d$. The nonlinear data overlap with the LVE envelope line very well at $Wi_0 < 30$ within experimental error, which confirms the validity of the Cox–Merz rule⁷⁰ for both linear and ring polymers. At higher shear rates, the nonlinear data are slightly lower than the linear envelope. The same observation has been reported for linear⁴² and comb polymers.^{43,44} This deviation may reflect a failure of this empirical rule or could be tentatively attributed to onset of weak wall slip or edge fracture propagating up to the gap between partition and cone of the CPP (although this is not supported by the long-time steady viscosity data in Figure 5). These possibilities have been discussed in detail recently.^{42–44} Nevertheless, it is reasonable to conclude that the empirical Cox–Merz rule is valid for ring polymers. We also note that the η_{STEADY} data for entangled linear PS ($Z = 5$ and 11) overlap within error over the whole Wi range and share the shear thinning slope of -0.86 ± 0.03 . The $\eta_{\text{STEADY}}/\eta_0$ data of the ring polymer overlap with those of the linear at low Wi in the linear (Newtonian) regime and deviate at higher values Wi . The weaker shear-thinning slope (-0.43 ± 0.03) resembles behavior akin to unentangled chains with finite extensibility.^{31–33} The data of the ring–linear 84k mixture are very close to those of entangled linear polymers, but not identical, especially for the lightly weaker shear thinning slope (-0.79 ± 0.01). That implies the addition of 15% rings can efficiently influence the nonlinear shear thinning behavior of linear matrix.

Figure 7b depicts the relative viscosities $\eta_{\text{MAX}}/\eta_{\text{STEADY}}$ as functions of Wi . Experimental errors are associated with torque resolution at low shear rates and start-up of the motor at high shear rates. The transient viscosity reduction after its peak toward steady state reflects chain retraction (manifested as partial disentanglement or tumbling) and the parameter $\eta_{\text{MAX}}/\eta_{\text{STEADY}}$ is the measure of the effective chain deformation at steady state. The data show its progressive increase with

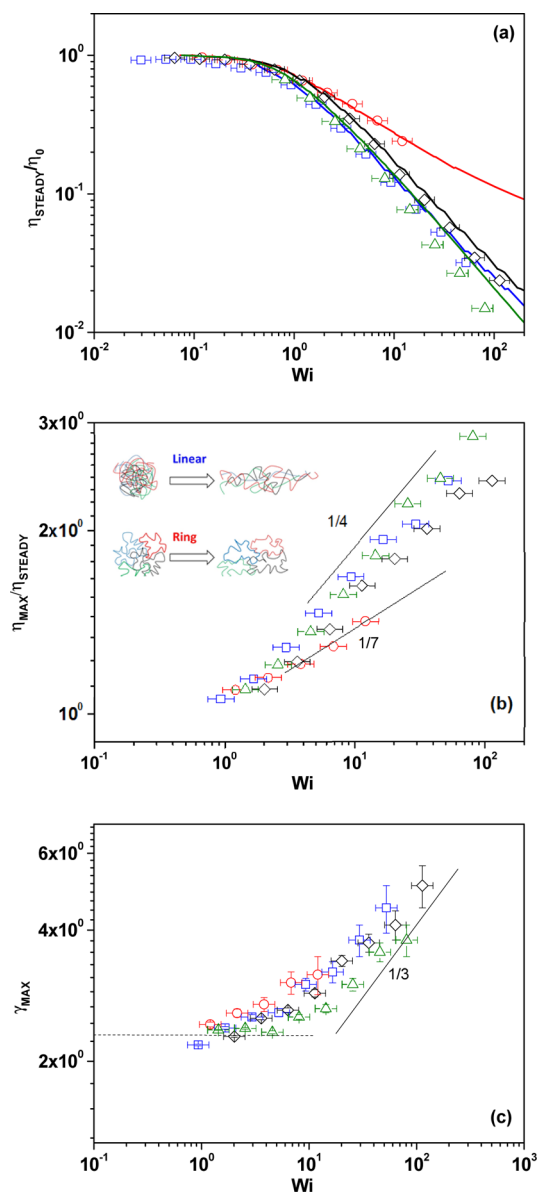


Figure 7. (a) Steady viscosity normalized with the zero-shear viscosity $\eta_{\text{STEADY}}/\eta_0$, (b) maximum viscosities scaled with steady viscosity $\eta_{\text{MAX}}/\eta_{\text{STEADY}}$, and (c) strains where the maxima occurs γ_{MAX} as a function of the Weissenberg number, Wi . Blue squares, red circles, black diamonds, and green triangles represent the PS-84k linear, PS-84k ring, their mixture with $\phi_L = 85\%$, and PS-185k linear, respectively. In (a), the blue, red, black, and green lines represent the respective complex viscosities (scaled with zero-shear viscosity) as a function of angular frequency (multiplied by τ_d) as calculated from the linear data for four samples. The cartoons in (b) illustrate the linear and ring chains at equilibrium, left, and large steady-state deformation (high Wi), right. The solid lines with slopes of 1/4 and 1/7, for the $\eta_{\text{MAX}}/\eta_{\text{STEADY}}$ evolution of linear and ring chains, respectively, are drawn to guide the eye. In (c), the solid line with a slope of 1/3 and the dashed horizontal line through $\gamma_{\text{MAX}} = 2.3$ are drawn to guide the eye (see text).

increasing Wi . In fact, for $Wi < 1$, i.e. in the linear regime where practically no viscosity peak occurs, $\eta_{\text{MAX}}/\eta_{\text{STEADY}}$ linear and ring polymers are rate-independent and assume a value of 1. Indeed, in this regime linear and ring chains are not expected to be deformed. For $Wi > 1$, the data of entangled linear PS collapse and follow a power-law with a scaling slope of 1/4,

which is also observed in other linear polymers in our previous works.⁴² On the other hand, the 84k ring data deviate from the linear data and exhibit weaker shear rate dependence with a slope about 1/7. This observation implies that the effective deformation of rings is smaller compared to linear chains, again in agreement with literature on single rings.³⁶ Like in Figure 7a, the data of the ring/linear mixture are in-between again with a slope of 1/5, pointing to the role of rings in altering linear chain nonlinear dynamics. The cartoon of Figure 7b attempts at depicting the situation. In steady shear flow, at sufficiently high rates, linear coils deform (and partly disentangle^{73,74}) much more efficiently than rings. The cartoon is exaggerated in order to clearly make the point of the different behavior, which is in line with the recent single molecule studies of DNA rings in solution³⁶ (although again we note that the present situation differs from the single molecule study).

Figure 7c depicts the strains at the peak viscosities, γ_{MAX} , as functions of the Weissenberg number, Wi . The errors on γ_{MAX} are obtained by simply multiplying the shear rate with the maximum time resolution of the standard data acquisition of the ARES (0.01 s). All three data sets overlap within experimental error. We note that γ_{MAX} denotes the maximum instantaneous deformation whereas $\eta_{\text{MAX}}/\eta_{\text{STEADY}}$ is proportional to the maximum deformation at steady state; hence, they differ in their sensitivity to molecular structure. The peak strain γ_{MAX} is between 2.0 and 2.3 at $Wi < 10$, consistent with observations in the literature^{42,75–77} and the Doi–Edwards model⁷⁸ for linear monodisperse polymers, which predicts that γ_{MAX} is due to orientation of the tube and attains a shear rate-independent value of 2.3. At higher Wi , the combination of both chain stretch and orientation governs the overshoot; hence, γ_{MAX} is expected to increase with Wi . The peak strain γ_{MAX} increases gradually with shear rate, and the high- Wi scaling slope is 1/3, consistent with the observation from a group of linear polymers^{42,79} but still lower than the steeper slope (= 1) predicted by the GLaMM theory.⁸⁰ Recently, Schweizer was able to predict a 1/3 slope for entangled linear polymers based on the idea that for a Weissenberg number larger than 1 based on Rouse time, chain retraction requires a minimum internal force to happen and correlates with the overshoot strain.^{81,82}

For linear polymers, the idea of convective constraint release (CCR)^{83,84} has proven to be an effective molecular mechanism to describe the nonlinear start-up shear flow behavior with good accuracy.^{77,80,85} For branched polymers like combs,^{43,44} a nonlinear hierarchical deformation scenario, including a short time branch withdrawn and a long time backbone orientation and stretch, drawn from the pom-pom model,^{86,87} was found to provide a reasonable description of nonlinear shear response. On the other hand, a molecular understanding of the nonlinear deformation of ring chains is still absent. One can advocate the double-folded ring conformation as a prime reason for their weak deformability. In other words, compared to their linear precursors, ring polymers have less freedom to change their conformation under shear flow because of their more compact structure. Additionally, the cooperative motion of ring segments under shear flow appears to be different from that of linear chains. Ring-specific dynamic mechanisms, such as cooperative orientation of parallel segments or the tumbling of segments, may account for the weak chain deformation under flow. In fact, recent simulations for small isolated rings (with number of Kuhn segments $N = 60, 80$, and 120 , i.e., the latter being almost identical to PS-84k with $N \approx 117$) in solution

indicate different tumbling behavior compared to linear polymers.^{34,35} More importantly, they show that finite extensibility is important for shear thinning with slope of -0.40 , which is very close to the present value of -0.43 . Whereas the present experimental system is different from simulations (marginal melt in the entanglement transition) and therefore this agreement should be taken as a full explanation, nevertheless this suggests that finite extensibility is at work here and rings indeed exhibit a weaker response to shear flow. Of course, one would qualitatively anticipate this result based on the weaker LVE behavior (Figure 3).

3.3. Nonlinear Stress Relaxation. The response to an imposed step strain deformation reflects the linear viscoelastic properties when the deformation is small. For larger deformations, which might induce conformational changes, the response becomes nonlinear and depends on the magnitude of the imposed strain. Nonlinear step strain measurements have been widely used to probe the chain behavior at large deformation^{45–49} and illustrate the different response between polymeric architectures.^{49,51,52} In such a deformation, the nonlinear moduli $G(t, \gamma)$ can be factorized as the product of two independent parts: the linear stress relaxation moduli, $G(t)$, and a strain-dependent function, $h(\gamma)$:

$$G(t, \gamma) = G(t)h(\gamma) \quad (6)$$

The vertical shift (ratio of nonlinear to linear strain) factor $h(\gamma)$ is called the “damping function” and physically represents that amount of stress that is to relax linearly (at the given strain).^{45,88} At linear regime with small strain, the damping function equals a constant of 1. After nonlinear large strains, a linear chain retracts rapidly, while the remaining stress (after retraction) will relax by slower (linear and nonlinear) processes. This remaining stress after rapid retraction is in fact the damping function.

The stress relaxation moduli after different step shear strains were measured at 150 °C for the marginally entangled linear and ring PS-84k. For comparison, a highly entangled blend of PS-198k ring and PS-450k linear with the fraction of the latter being 0.001 was measured at 170 °C. Its linear viscoelastic response is provided for completeness in the Supporting Information (Figure S1). After vertical shifting at different strains (see Figures S2 and S3), the moduli collapse onto the LVE envelope, suggesting the success of time-strain separability for both linear and ring polymers as well as the blend. The damping functions for three samples are plotted as a function of strain in Figure 8. The data are compared with the Doi–Edwards (DE) prediction⁶⁸ for well-entangled linear polymers:

$$h(\gamma) = \frac{1}{1 + \frac{4}{15}\gamma^2} \quad (7)$$

Note that the prefactor of $4/15$ used in the above equation represents the prediction without the independent alignment approximation.^{51,52,89–93} The damping functions of the linear polymer are γ -independent at low- γ and then decrease at large- γ . This shear thinning of the PS-84k linear is weaker than the DE prediction. This is attributed to the fact that this polymer is only moderately entangled.⁵¹ Note that the Rouse model predicts damping functions for an unentangled linear or ring chain is constant ($h(\gamma) = 1$);^{32,68} however, finite extensibility induces thinning,³³ as already discussed above. Therefore, it is natural that the damping functions of the ring polymer thin at large strains but exhibit a weaker strain dependence than linear

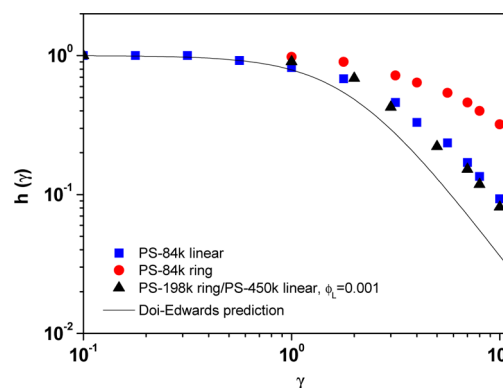


Figure 8. Comparison of damping functions between the PS-84k linear (blue squares) and the PS-84k ring (red squares). Also plotted are data of the ring/linear mixture PS-198k ring/PS-450k linear with linear fraction $\phi_L = 0.001$ (see text). The solid line is the prediction of Doi–Edwards theory (see text).

chains. On the other hand, for the large molar mass PS-198k ring/PS-450k linear blends, the damping functions are virtually identical to those of the moderate entangled PS-84k linear chains, reflecting the network-like structure of the blend due to the rings penetration by linear chains. Despite the comparison to entangled and unentangled chains with finite extensibility, the different (more compact) shape of small rings (with respect to large ring or linear chains), and the good agreement with available simulations and single-ring extensional deformation data, a rationalization of the nonlinear rheology of rings remains a challenge. We hope that the present data will trigger more experimental and modeling/simulation work in this direction. Clearly, larger molar mass polymers should be considered as well.

4. CONCLUDING REMARKS

In this work, we have presented linear and nonlinear rheological data of a marginally entangled, experimentally pure ring polymer. The linear viscoelasticity shows the established power-law stress relaxation, however with an exponent larger than 0.4, predicted by the lattice-animal model. Both this and the Rouse-ring model capture frequency-dependent moduli, with the latter slightly underestimating the terminal relaxation. The slow relaxation is not captured by either model, as expected, and is attributed to interactions of rings with unlinked linear chains and possibly other rings. The overshoot in transient viscosity of the ring at high Weissenberg numbers, is less prominent compared to its linear precursor, suggesting that the nonlinear deformation of rings is weaker compared to their linear counterparts. This is also reflected in their weaker shear thinning behavior as well as their weaker damping function in step-strain experiments. Complementary data obtained with ring–linear blends exhibit a nonlinear shear behavior closer to that of entangled linear chains and confirm the emerging picture. Available fragmental information from single DNA ring extensional deformation and molecular simulations of sheared single ring in solution provide further evidence for the weaker ring deformation and the importance of finite extensibility, especially for small molecular weights. The present data set should motivate further shear and extensional experiments with larger molecular weights and mixtures as well as theoretical developments in this exciting field of research.

■ ASSOCIATED CONTENT**■ Supporting Information**

The Supporting Information is available free of charge on the ACS Publications website at DOI: 10.1021/acs.macromol.5b02651.

Figures S1–S3 (PDF)

■ AUTHOR INFORMATION**Corresponding Author**

*E-mail dvlasso@iesl.forth.gr (D.V.).

Notes

The authors declare no competing financial interest.

■ ACKNOWLEDGMENTS

This work was supported by the Greek General secretariat for Research and Technology (program ESPA Aristeia-Rings). T.C. acknowledges the support from NRF-Korea (2015R1A2A2A01004974). We thank M. Kapnistos for the measurements with the PS-198k ring/PS-450k linear blend and M. Rubinstein for enlightening discussions.

■ REFERENCES

- (1) Kapnistos, M.; Lang, M.; Vlassopoulos, D.; Pyckhout-Hintzen, W.; Richter, D.; Cho, D.; Chang, T.; Rubinstein, M. *Nat. Mater.* **2008**, *7*, 997–1002.
- (2) Pasquino, R.; Vasilakopoulos, T. C.; Jeong, Y. C.; Lee, H.; Rogers, S.; Sakellariou, G.; Allgaier, J.; Takano, A.; Brás, A. R.; Chang, T.; Gooßen, S.; Pyckhout-Hintzen, W.; Wischniewski, A.; Hadjichristidis, N.; Richter, D.; Rubinstein, M.; Vlassopoulos, D. *ACS Macro Lett.* **2013**, *2*, 874–878.
- (3) Halverson, J. D.; Lee, W. B.; Grest, G. S.; Grosberg, A. Y.; Kremer, K. *J. Chem. Phys.* **2011**, *134*, 204904.
- (4) Halverson, J. D.; Lee, W. B.; Grest, G. S.; Grosberg, A. Y.; Kremer, K. *J. Chem. Phys.* **2011**, *134*, 204905.
- (5) Doi, Y.; Matsubara, K.; Ohta, Y.; Nakano, T.; Kawaguchi, D.; Takahashi, Y.; Takano, A.; Matsushita, Y. *Macromolecules* **2015**, *48*, 3140–3147.
- (6) Gooßen, S.; Brás, A. R.; Krutyeva, M.; Sharp, M.; Falus, P.; Feoktystov, A.; Gasser, U.; Pyckhout-Hintzen, W.; Wischniewski, A.; Richter, D. *Phys. Rev. Lett.* **2014**, *113*, 168302.
- (7) Vlassopoulos, D.; Pasquino, R.; Sijm, F. In *Topological Polymer Chemistry: Progress of Cyclic Polymers in Synthesis, Properties and Functions*; Tezuka, Y., Ed.; World Scientific Publishing: London, 2012.
- (8) McLeish, T. *Nat. Mater.* **2008**, *7*, 933–935.
- (9) Roovers, J. *Macromolecules* **1985**, *18*, 1359–1361.
- (10) Roovers, J. *Macromolecules* **1988**, *21*, 1517–1521.
- (11) McKenna, G.; Plazek, D. *Psychosomatics* **1986**, *27*, 304–306.
- (12) Orrah, D.; Semlyen, J.; Ross-Murphy, S. *Polymer* **1988**, *29*, 1452–1454.
- (13) Lee, H. C.; Lee, H.; Lee, W.; Chang, T.; Roovers, J. *Macromolecules* **2000**, *33*, 8119–8121.
- (14) Rubinstein, M. *Phys. Rev. Lett.* **1986**, *57*, 3023–3026.
- (15) Cates, M.; Deutsch, J. *J. Phys. (Paris)* **1986**, *47*, 2121–2128.
- (16) Obukhov, S. P.; Rubinstein, M.; Duke, T. *Phys. Rev. Lett.* **1994**, *73*, 1263–1266.
- (17) Ge, T.; Panyukov, S.; Rubinstein, M. Submitted to *Macromolecules*.
- (18) Milner, S. T.; Newhall, J. D. *Phys. Rev. Lett.* **2010**, *105*, 208302.
- (19) Grosberg, A. Y. *Soft Matter* **2014**, *10*, 560–565.
- (20) Obukhov, S.; Johner, A.; Baschnagel, J.; Meyer, H.; Wittmer, J. *Europhys. Lett.* **2014**, *105*, 48005.
- (21) Rosa, A.; Everaers, R. *Phys. Rev. Lett.* **2014**, *112*, 118302.
- (22) Tsalikis, D. G.; Mavrantzas, V. G. *ACS Macro Lett.* **2014**, *3*, 763–766.
- (23) Halverson, J. D.; Grest, G. S.; Grosberg, A. Y.; Kremer, K. *Phys. Rev. Lett.* **2012**, *108*, 038301.
- (24) Chang, T. *J. Polym. Sci., Part B: Polym. Phys.* **2005**, *43*, 1591–1607.
- (25) Deutman, A. B.; Monnereau, C.; Elemans, J. A.; Ercolani, G.; Nolte, R. J.; Rowan, A. E. *Science* **2008**, *322*, 1668–1671.
- (26) Lo, W. C.; Turner, M. S. *Europhys. Lett.* **2013**, *102*, S8005.
- (27) Michieletto, D.; Marenduzzo, D.; Orlandini, E.; Alexander, G. P.; Turner, M. S. *ACS Macro Lett.* **2014**, *3*, 255–259.
- (28) Lee, E.; Kim, S.; Jung, Y. *Macromol. Rapid Commun.* **2015**, *36*, 1115–1121.
- (29) Watanabe, H.; Inoue, T.; Matsumiya, Y. *Macromolecules* **2006**, *39*, 5419–5426.
- (30) Likhtman, A. E.; McLeish, T. C. B. *Macromolecules* **2002**, *35*, 6332–6343.
- (31) Carl, W. J. *Chem. Soc., Faraday Trans.* **1995**, *91*, 2525–2530.
- (32) Wiest, J. M.; Burdette, S. R.; Liu, T. W.; Bird, R. B. *J. Non-Newtonian Fluid Mech.* **1987**, *24*, 279–295.
- (33) Cifre, J. H.; Pamies, R.; Martínez, M. L.; De La Torre, J. G. *Polymer* **2005**, *46*, 267–274.
- (34) Chen, W.; Li, Y.; Zhao, H.; Liu, L.; Chen, J.; An, L. *Polymer* **2015**, *64*, 93–99.
- (35) Chen, W.; Chen, J.; An, L. *Soft Matter* **2013**, *9*, 4312–4318.
- (36) Li, Y.; Hsiao, K.-W.; Brockman, C. A.; Yates, D. Y.; Robertson-Anderson, R. M.; Kornfield, J. A.; San Francisco, M. J.; Schroeder, C. M.; McKenna, G. B. *Macromolecules* **2015**, *48*, 5997–6001.
- (37) Larson, R. G. *Rheol. Acta* **1992**, *31*, 213–263.
- (38) Meissner, J.; Garbella, R.; Hostettler, J. *J. Rheol.* **1989**, *33*, 843–864.
- (39) Schweizer, T. *J. Rheol.* **2003**, *47*, 1071–1085.
- (40) Li, X.; Wang, S.-Q. *Rheol. Acta* **2010**, *49*, 985–991.
- (41) Schweizer, T.; Schmidheiny, W. *J. Rheol.* **2013**, *57*, 841–856.
- (42) Sijm, F.; Vlassopoulos, D. *J. Rheol.* **2011**, *55*, 1167–1186.
- (43) Sijm, F.; Vlassopoulos, D.; Lee, H.; Yang, J.; Chang, T.; Driva, P.; Hadjichristidis, N. *J. Rheol.* **2013**, *57*, 1079–1100.
- (44) Sijm, F.; Vlassopoulos, D.; Ianniruberto, G.; Marrucci, G.; Lee, H.; Yang, J.; Chang, T. *ACS Macro Lett.* **2013**, *2*, 601–604.
- (45) Rolón-Garrido, V. H.; Wagner, M. H. *Rheol. Acta* **2009**, *48*, 245–284.
- (46) Islam, M. T.; Sanchez-Reyes, J.; Archer, L. A. *Rheol. Acta* **2003**, *42*, 191–198.
- (47) Archer, L. A.; Sanchez-Reyes, J.; Juliani. *Macromolecules* **2002**, *35*, 10216–10224.
- (48) Iza, M.; Bousmina, M. *Rheol. Acta* **2005**, *44*, 372–378.
- (49) Lee, J. H.; Fetters, L. J.; Archer, L. A. *Macromolecules* **2005**, *38*, 10763–10771.
- (50) McLeish, T.; Allgaier, J.; Bick, D.; Bishko, G.; Biswas, P.; Blackwell, R.; Blottiere, B.; Clarke, N.; Gibbs, B.; Groves, D. *Macromolecules* **1999**, *32*, 6734–6758.
- (51) Kapnistos, M.; Kirkwood, K. M.; Ramirez, J.; Vlassopoulos, D.; Leal, L. G. *J. Rheol.* **2009**, *53*, 1133–1153.
- (52) Kirkwood, K. M.; Leal, L. G.; Vlassopoulos, D.; Driva, P.; Hadjichristidis, N. *Macromolecules* **2009**, *42*, 9592–9608.
- (53) Hirao, A.; Higashihara, T.; Nagura, M.; Sakurai, T. *Macromolecules* **2006**, *39*, 6081–6091.
- (54) Takano, A.; Nonaka, A.; Kadoi, O.; Hirahara, K.; Kawahara, S.; Isono, Y.; Torikai, N.; Matsushita, Y. *J. Polym. Sci., Part B: Polym. Phys.* **2002**, *40*, 1582–1589.
- (55) Cho, D.; Park, S.; Kwon, K.; Chang, T.; Roovers, J. *Macromolecules* **2001**, *34*, 7570–7572.
- (56) Lee, W.; Lee, H.; Cha, J.; Chang, T.; Hanley, K. J.; Lodge, T. P. *Macromolecules* **2000**, *33*, 5111–5115.
- (57) Macosko, C. W.; Larson, R. G. *Rheology: Principles, Measurements, and Applications*; Wiley: New York, 1994.
- (58) Schweizer, T. *Rheol. Acta* **2002**, *41*, 337–344.
- (59) Kapnistos, M.; Vlassopoulos, D.; Roovers, J.; Leal, L. *Macromolecules* **2005**, *38*, 7852–7862.
- (60) Roovers, J.; Toporowski, P. *Macromolecules* **1981**, *14*, 1174–1178.

- (61) Roovers, J. *Macromolecules* **1984**, *17*, 1196–1200.
- (62) Ferry, J. D. *Viscoelastic Properties of Polymers*, 3rd ed.; Wiley: New York, 1980.
- (63) Walsh, D.; Zoller, P. *Standard Pressure Volume Temperature Data for Polymers*; CRC Press: 1995.
- (64) Inoue, T.; Okamoto, H.; Osaki, K. *Macromolecules* **1991**, *24*, 5670–5675.
- (65) Inoue, T.; Matsui, H.; Osaki, K. *Rheol. Acta* **1997**, *36*, 239–244.
- (66) Larson, R. G.; Sridhar, T.; Leal, L. G.; McKinley, G. H.; Likhtman, A. E.; McLeish, T. C. B. *J. Rheol.* **2003**, *47*, 809–818.
- (67) Harmandaris, V.; Mavrantzas, V.; Theodorou, D.; Kröger, M.; Ramirez, J.; Öttinger, H.; Vlassopoulos, D. *Macromolecules* **2003**, *36*, 1376–1387.
- (68) Doi, M.; Edwards, S. F. *The Theory of Polymer Dynamics*; Clarendon Press: Oxford, UK, 1986.
- (69) McKenna, G. B.; Hostetter, B. J.; Hadjichristidis, N.; Fetters, L. J.; Plazek, D. J. *Macromolecules* **1989**, *22*, 1834–1852.
- (70) Cox, W. P.; Merz, E. H. *J. Polym. Sci.* **1958**, *28*, 619–622.
- (71) Gleissle, W. In *Rheology*; Astarita, G., Marrucci, G., Nicolais, L., Eds.; Plenum: New York, 1980; Vol. 2, p 457.
- (72) Rubinstein, M.; Colby, R. H. *Polymer Physics*; Oxford University Press: Oxford, UK, 2003.
- (73) Ianniruberto, G.; Marrucci, G. *J. Rheol.* **2014**, *58*, 89–102.
- (74) Baig, C.; Mavrantzas, V. G.; Kröger, M. *Macromolecules* **2010**, *43*, 6886–6902.
- (75) Menezes, E.; Graessley, W. J. *Polym. Sci., Polym. Phys. Ed.* **1982**, *20*, 1817–1833.
- (76) Schweizer, T.; van Meerveld, J.; Ottinger, H. C. *J. Rheol.* **2004**, *48*, 1345–1364.
- (77) Auhl, D.; Ramirez, J.; Likhtman, A. E.; Chambon, P.; Fernyhough, C. *J. Rheol.* **2008**, *52*, 801–835.
- (78) Doi, M.; Edwards, S. J. *Chem. Soc., Faraday Trans. 2* **1979**, *75*, 38–54.
- (79) Ravindranath, S.; Wang, S.-Q. *J. Rheol.* **2008**, *52*, 681–695.
- (80) Graham, R. S.; Likhtman, A. E.; McLeish, T. C.; Milner, S. T. *J. Rheol.* **2003**, *47*, 1171–1200.
- (81) Schweizer, K. S. Private communication, 2015.
- (82) Wang, S. Q.; Ravindranath, S.; Wang, Y. Y.; Boukany, P. Y. *J. Chem. Phys.* **2007**, *127*, 064903.
- (83) Graessley, W. W. *J. Chem. Phys.* **1965**, *43*, 2696–2703.
- (84) Marrucci, G. *J. Non-Newtonian Fluid Mech.* **1996**, *62*, 279–289.
- (85) Pearson, D.; Herbolzheimer, E.; Grizzuti, N.; Marrucci, G. *J. Polym. Sci., Part B: Polym. Phys.* **1991**, *29*, 1589–1597.
- (86) McLeish, T.; Larson, R. *J. Rheol.* **1998**, *42*, 81–110.
- (87) Marrucci, G.; Ianniruberto, G.; Bacchelli, F.; Coppola, S. *Prog. Theor. Phys. Suppl.* **2008**, *175*, 1–9.
- (88) Wagner, M. *Rheol. Acta* **1976**, *15*, 136–142.
- (89) Larson, R. *J. Rheol.* **1984**, *28*, 545–571.
- (90) Larson, R. *J. Rheol.* **1985**, *29*, 823–831.
- (91) Takahashi, M.; Isaki, T.; Takigawa, T.; Masuda, T. *J. Rheol.* **1993**, *37*, 827–846.
- (92) Kasehagen, L. J.; Macosko, C. W. *J. Rheol.* **1998**, *42*, 1303–1327.
- (93) Venerus, D. C. *J. Rheol.* **2005**, *49*, 277–295.